Ab Initio Molecular Dynamics Study of Uracil in Aqueous Solution

Marie-Pierre Gaigeot*

Laboratoire de Modelisation des Systemes Moleculaires Complexes, Université d'Evry val d'Essonne, Rue Pere A Jarland, F-91025, France

Michiel Sprik*

Department of Chemistry, University of Cambridge, Lensfield Road, CB2 1EW, United Kingdom

Received: January 6, 2004; In Final Form: March 24, 2004

The hydrogen bonding of uracil in aqueous solution is investigated using density functional based ab initio molecular dynamics simulation ("Car−Parrinello"). During the 7 ps trajectory, the solute was observed to be coordinated by a first hydration shell composed of up to nine water molecules. Six water molecules are hydrogen-bonded to the amide and carbonyl groups and three further water molecules are located on either side of the uracil ring with a tendency to approach the ring through π-hydrogen bonding. The hydrogen bonding is characterized by the computation of a number of structural and dynamical correlation functions. To highlight the importance of the finite temperature bulk solvent, these results are compared to structures obtained by a number of previous structural studies of ground-state hydrated clusters. The analysis presented here is the structural complement to an ab initio molecular dynamics determination of the infrared absorption spectrum of aqueous uracil that has appeared as a separate publication (*J. Phys. Chem. B* **2003**, *107*, 10344).

1. Introduction

The affinity of organic molecules for hydrogen bonding is mainly (but not exclusively) determined by oxygen- or nitrogen-containing functional groups (such as hydroxyl, carbonyl, amine, and amide groups). Hydrogen bonding to water is of special interest in view of the biological function of some of these molecules. The number and strength of hydrogen bonds formed with water depend on several factors, such as atomic charges, and accessibility of a site. These essential aspects of hydrogen bonding are adequately covered by classical point charge models as incorporated in molecular dynamics simulation packages. These partly empirical models have reached the stage where they can give a quantitative picture of solvation and therefore, indirectly, can explain a number of further properties such as the conformation of flexible molecules in solution (because of the relevance to the topic of this paper, we mention here some examples of the applications to nucleic acids[1−8]). Classical simulations confirm that hydrogen bonding to hydrophilic sites (the first solvation shell) can be rather specific. Atomistic pictures of hydration represent a unique contribution of computation to the field of structural biology as such details are not easily accessible to direct structural probes. Often experimental information is only available indirectly from the effect of solvent on spectroscopic properties such as infrared, Raman, or magnetic spectra. Since many of the vibrational modes in hydrophilic groups are infrared-active, infrared absorption is particularly sensitive to hydrogen bonding. However, while structure and energetics of the solvation shell may be correctly reproduced, standard classical force field models are not suitable for computation of infrared absorption. The crucial element missing is electronic polarization. Designing polarizable force fields that can be used to compute infrared intensities is possible[9] but not straightforward.

Electronic polarization is accounted for at a fundamental level in the density functional based ab initio molecular dynamics ("Car−Parrinello") method.[10] The infrared absorption of a liquid can therefore in principle be obtained directly from the Fourier transform of the polarization time correlation as computed from the MD trajectory. However, a fundamental difficulty stood in the way of this "natural" application of ab initio MD, namely a proper determination (definition) of polarization in periodic systems. After this problem had been resolved in the early 1990s by Vanderbilt and co-workers,[11,12] Silverstrelli et al.[13] were the first to exploit this development in an ab initio MD study of the infrared absorption of liquid water, with good results (for an application to an aqueous KOH solution, see ref 14). In a previous publication[15] (hence forward referred to as paper I) which appeared in a recent issue of this journal, we have extended this approach to the infrared spectrum of an organic aqueous solute, namely uracil (one of the nucleic acid bases). The computed spectral patterns of the molecule immersed in liquid water were in remarkably good agreement with experiment, which enabled us to analyze the solvent effect by comparison with the gas-phase spectrum obtained using a similar dynamical methodology. The observed shift and broadening of the lines could be interpreted in terms of the hydrogen bonding between uracil and surrounding water molecules. The technical discussion in paper I was focused on calculation and interpretation of the infrared spectrum, such as separation of solute and solvent signal, assignment, and quantum corrections. Analysis of the hydrogen bonding was restricted to those structural features relevant for the interpretation of the spectrum. A more comprehensive analysis of the hydrogen bonding of aqueous uracil was deferred. This is the subject of the present publication.

A detailed investigation of a representative organic aqueous solute such as uracil also serves a more technical purpose,

* Corresponding authors. E-mail: (M.P.G.) gaigeot@ccr.jussieu.fr and (M.S.) ms284@cam.ac.uk.

10.1021/jp049940m CCC: $27.50
Published on Web 05/12/2004

namely further validation of the "Car−Parrinello model" in aqueous chemistry. A key requirement for molecular dynamics simulation of aqueous systems is that the length of the dynamical trajectories is sufficient to equilibrate and sample the essential thermal fluctuations of hydrogen-bonded liquids and solutions. Measured on this time scale, the run lengths in ab initio MD (currently limited to the 10−20 ps time scale) are rather short. In addition, liquids are disordered; hence, also the size of model systems is a critical parameter. Errors introduced by limitations in run length and system size are therefore intertwined, because an increase in system dimensions in general imposes further restrictions on the time scale of the run. The question about accuracy is further compounded by uncertainties with regard to the performance DFT methods for hydrogen bonding, as it appears that results of computations for small clusters in a vacuum are not easily transferable to the bulk. The consequence of all these complications is that the hydration of solute species needs continuous, almost case-by-case testing under bulk conditions. Uracil, exposing a variety of hydrogen-bonding sites to the solvent, is an excellent target for such a test.

Organization of this paper is as follows. We start with a brief overview of the results of gas-phase hydration studies based on electronic structure calculation (section 2), followed by an outline of various aspects of the computational methodology used in this paper (section 3). Results for the structure of aqueous uracil are discussed in section 4. We computed statistical distributions and correlations for a variety of geometric characteristics describing hydrogen bonding. Section 5 is devoted to relaxation dynamics (diffusion and reorientation). We conclude with a comparison to gas-phase hydration (section 6) and a summary (section 7) where we also return to the issue of performance of ab initio MD methods for aqueous systems.

2. Gas-Phase Hydration Studies

Geometry and energetics of nucleic bases interacting with a small number of water molecules in the gas phase have been the subject of several electronic calculations since the pioneering investigations of Pullman et al.[16,17] and del Bene.[18] The past few years showed a renewal of interest, stimulated by the continuous increase of computer hardware performance, extending the calculations to more realistic hydrated complexes at increasing levels of precision. The latest studies consisted of ab initio geometry optimizations of small clusters composed of a nucleic acid base (uracil, thymine, cytosine, adenine, or guanine) surrounded by a few explicit water molecules.[19−38]

Uracil, as the structurally most simple nucleic acid base, has received a great deal of attention. Recent examples are detailed geometry optimizations of uracil•$n_w$$H_2O$ complexes.[21−23,28−31,35,37,38] In these studies, the number of water molecules, n_w, varies from 1 to 7. Different theoretical levels of calculation (HF, MP2, and DFT) have been considered and their results compared. The uracil•H_2O complex[21,22,28−30,35,37,38] has been a major focus, in particular the determination of the hydrophilic sites that are energetically the most favorable for hydrogen bonding to the water molecule. Calculations involving several water molecules in a variety of arrangements[23,31,35,37,38] have also been carried out in order to gain detailed insight into the structural patterns adopted by water molecules around uracil.

In a previous study using geometry optimization methods, we showed that up to seven water molecules can be hydrogen bonded to the main hydrophilic sites of uracil.[37,38] The location of the molecules was constrained in this calculation to the plane defined by the base ring. Neither out-of-plane hydration nor the effect of water molecules in the second hydration shell was considered. Recognizing that the three-dimensional nature of the H-bonded network could be of importance, Gadre et al.[35] have optimized configurations in which up to 15 water molecules were placed around uracil, representing part of the first and second hydration shells. To treat a system of this size, an electrostatic-based model (EPIC) was employed. Still, the number of possible arrangements of the uracil•$15H_2O$ complex is already sufficiently large to make locating the global minimum of the potential energy surface not an easy task. The complications obviously multiply with addition of further water molecules, preventing a complete description of the different solvation shells. However, while of interest for the understanding of the nature of hydrogen-bonding interactions, it is questionable whether the level of detail provided by full geometry optimization is necessary or even sufficient when the goal is to describe the hydration by finite-temperature bulk solvents. This is the perspective offered by the Car−Parrinello method.

3. Computational Methodology: Outline

Ab initio Molecular Dynamics Method. The Car−Parrinello (CP) approach combines plane wave-pseudopotential methods for the determination of the electronic structure of extended systems with the generalized gradient approximation (GGA) developed for treating molecules. A special feature distinguishing the CP method from other ab initio MD methods is the dynamical scheme for optimization of the electronic states based on the fictitious (classical) dynamics of the electronic degrees of freedom[10] (for a technical introduction to CP techniques, see ref 39). The technical implementation used in this work is the same as in previous ab initio MD studies of aqueous systems. After numerous validations, this setup has become standard for the application of the Car−Parrinello method to first row chemistry (see, however, section 7). The one-electron orbitals are expanded in a plane wave basis set, with a kinetic energy cutoff of 70 Ry restricted to the Γ point of the Brillouin zone. Medium soft norm-conserving pseudopotentials of the Martins−Trouillier type[40] are used. The core-valence interaction of C, N, and O is treated by *s* and *p* potentials with pseudization radii of 1.23 au, 1.12 au, 1.05 au, respectively (taking the same radius for *s* and *p*). Energy expectation values are computed in reciprocal space using the Kleinman−Bylander transformation.[41] Hydrogen atoms are represented by a simple *s* potential damping the Coulomb singularity at the origin. We used the Becke, Lee, Yang, and Parr (BLYP) [42,43] gradient corrected functional for the exchange and correlation terms.

Model System and MD Parameters. The system modeled in this work is composed of one uracil molecule surrounded by 49 water molecules (total number of 159 atoms, a computer graphics representation of this system can be found in paper I). The dimensions of the periodically repeated cubic cell are 11.5 Å in all three directions. With a solvent system of this size, two complete layers of solvent, and part of the third hydration shell around uracil, are taken into account. The simulations were performed at constant volume using a fictitious electron mass of 600 au and a time step of 5 au (0.12 fs). In the equilibration phase, the temperature was controlled by velocity scaling. The trajectory over which the data for the hydration analysis was collected is strictly microcanonical. The average ionic temperature obtained over the length of this run (7.3 ps) was 310 K. Exactly the same trajectory was used in paper I for the determination of the infra-absorption spectrum. Hydrogen atoms were treated as classical particles with their true mass (1836 au).

The choice of the exact number of molecules in a given MD cell is a question that needs careful consideration, since one

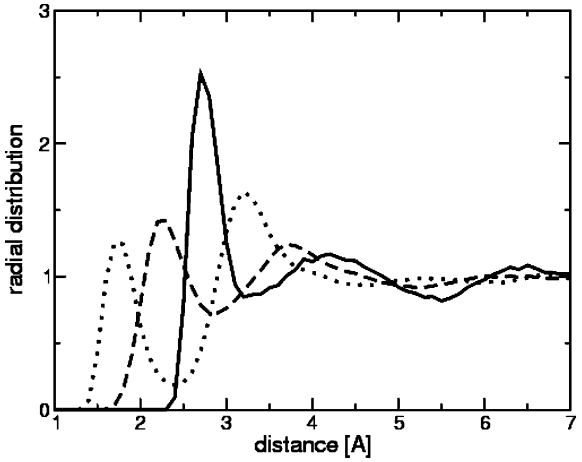

Figure 1. Radial pair distribution function (RDF) of water solvent calculated by averaging over the 7.3 ps molecular dynamics simulation of the uracil solution: $g_{OwOw}(r)$ (solid line), $g_{OwHw}(r)$ (dotted line), and $g_{HwHw}(r)$ (dashed line). Ow denotes oxygen atoms of water molecules and Hw hydrogen atoms.

TABLE 1: Positions r^{max} and r^{min} (Å) and Amplitudes g^{max} and g^{min} of the Maxima and Minima of the First Peaks of Uracil−Water (Figures 3−5) and Water−Water (Figure 1) Pair Correlation Functions

	H1−Ow	H3−Ow	O2−Hw	O4−Hw	Ow−Hw	Ow−Ow
r^{max}	1.80	1.80	1.80	1.80	1.70	2.70
g^{max}	1.06	1.00	1.15	1.36	1.26	2.50
r^{min}	2.50	2.40	2.50	2.30	2.40	3.20
g^{min}	0.37	0.17	0.24	0.25	0.18	0.85
g^{max}/g^{min}	2.9	5.9	4.8	5.5	7.0	3.0

[a] Labeling of solute atoms is according to Figure 2. Ow denotes water oxygen atoms, and Hw denotes water hydrogen atoms.

solvent molecule more or less can have a significant effect on the pressure in such small cells of fixed volume. We arrived at the number of 49 H_2O molecules, following the sample preparation procedure of ref 44. The cubic cell of 11.5 Å was first filled with water molecules only at ambient density of bulk liquid and the pressure was determined in a 500 ps run at a temperature of 300 K using standard classical force field MD. Next, a cluster of H_2O molecules was replaced by the solute (uracil) and the pressure recomputed. Taking the pressure of the pure water sample as the target, the number of water molecules was adjusted until this pressure was recovered. The final configuration of this classical simulation was then used as the starting point for the DFT-molecular dynamics. After a short reequilibration (0.5 ps), the data collection run was initiated. All simulations were carried out with version 3.4.1 of the CPMD ab initio molecular dynamic package.[45]

4. Structural Properties

Radial Pair Correlation Functions. Radial distribution functions are a good way of probing hydrogen bonding in solutions. We first investigated the solvent surrounding the uracil to see whether there are major differences with pure water. Figure 1 shows the usual water pair correlations, namely $g_{OwOw}(r)$, $g_{OwHw}(r)$, and $g_{HwHw}(r)$. They were calculated from the molecular dynamics simulation of the fully solvated uracil system. Table 1 summarizes relevant data for the first peak of $g_{OwOw}(r)$ and $g_{OwHw}(r)$ in numerical form. Hereafter, water oxygen's are denoted by Ow and water hydrogen's by Hw. All three curves are very similar to the structures obtained in the Car−Parrinello molecular dynamics simulations of pure liquid water[46,47] for a similar size system. In particular, g_{OwOw} displays

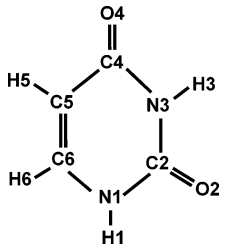

Figure 2. Schematic picture of uracil with labeling of atoms used in the text.

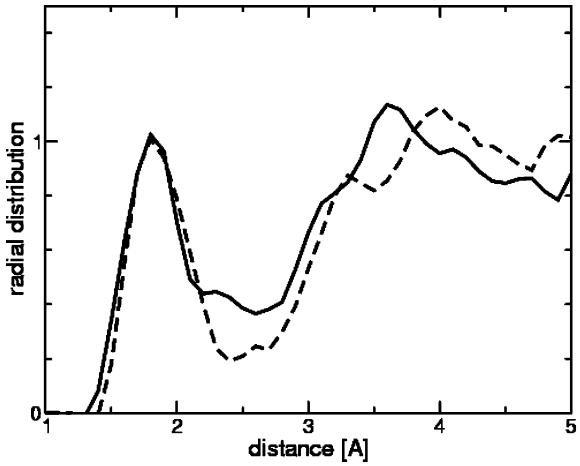

Figure 3. Radial pair correlation functions $g_{H1Ow}(r)$ (solid) and $g_{H3Ow}(r)$ (dashed) between uracil amide hydrogen atoms H1 and H3 (labeling of atoms is given in Figure 2) and water oxygen atoms Ow. See Table 1 for a numerical specification of position and height of first peaks.

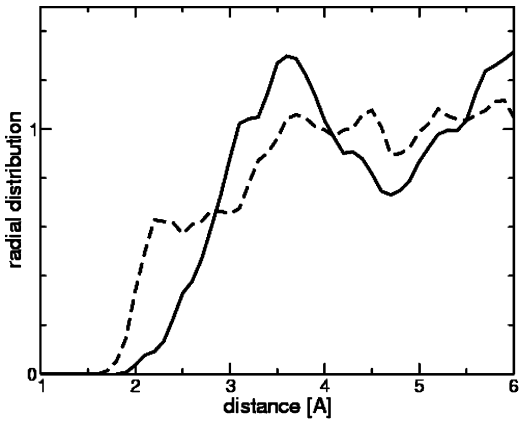

Figure 4. Radial pair correlation functions $g_{H5Ow}(r)$ (solid) and $g_{H6Ow}(r)$ (dashed) between uracil C−H hydrogen atoms H5 and H6 (see Figure 2) and water oxygen atoms. See also Table 1.

the familiar first maximum located at 2.70 Å (with amplitude $g^{max} = 2.50$; see Table 1) and first minimum at $r^{min} \sim 3.20$ Å (with amplitude $g^{min} = 0.85$). This peak, reflecting the hydrogen bonding to first neighbors, can be directly compared to the pure water result. We verified that each water molecule has a coordination number of $n_c \sim 4.30$, very close to the result of pure liquid water. The second peak of $g_{OwOw}(r)$ has a maximum located at ∼4.20 Å (amplitude 1.17) and a minimum at ∼5.50 Å (amplitude 0.82), again very similar to pure liquid water. This confirms that the intermolecular interactions in the water solvent, despite the small size of our model system, are not drastically disturbed by the presence of the solute.

Uracil−water atomic pair correlation functions are plotted in Figures 3−5. Figure 2 gives our convention for the labeling of atoms (identical labeling was used in paper I). Numerical

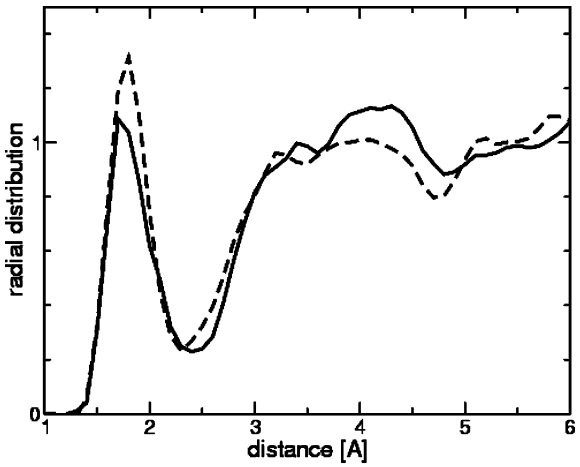

Figure 5. Radial pair correlation functions $g_{O2Hw}(r)$ (solid) and $g_{O4Hw}(r)$ (dashed) between uracil carbonyl oxygen atoms O2 and O4 (labeling according to Figure 2) and Hw hydrogen atoms of solvent. See also Table 1.

values for positions of maxima and minima (r^{max} and r^{min}, respectively) and amplitudes (g^{max} and g^{min}, respectively) can again be found in Table 1. We immediately note a strong difference between the radial distribution function (RDF) for H1−Ow and H3−Ow (Figure 3) on one hand and H5−Ow and H6−Ow (Figure 4) on the other hand. The RDF for H1(H3)−Ow has an overall structure very similar to the solvent oxygen-solvent hydrogen correlation of Figure 1. Accordingly, we can take the prominent first peak at short intermolecular distances as proof of the formation of stable hydrogen bonds between the solvent oxygen and H1 and H3 atoms of the solute. The second peak located at intermediate distances is then a manifestation of ordering of water molecules in a stable second hydration shell around uracil. Such characteristics are missing in the H5(H6)−Ow RDFs (Figure 4), confirming that H5 and H6 are essentially inactive for hydrogen bonding. Carbonyl oxygen's are in general good hydrogen bond acceptors, and indeed in the RDFs of Figure 5, describing the O2−Hw and O4−Hw correlations, we again recognize the regular first maximum at 1.80 Å and minimum at ∼2.30−2.50 Å characteristic of hydrogen bonds.

Number and Strength of Hydrogen Bonds. The well-defined maxima in the H1−Ow and H3−Ow radial distributions can be used to estimate the effective number of hydrogen bonds formed by these polar groups. If we take the integral of the curves up to the minimum at $r_c = r^{min} \sim 2.40-2.50$ Å (which also corresponds to the conventional maximum length of hydrogen bonds), we find coordination numbers of $n_{H1} = 1.0$ and $n_{H3} = 0.9$ respectively for H1 and H3 atoms, implying that H1 and H3 participate in one hydrogen bond, on average. Of special interest for the chemistry of aqueous nucleic bases are possible subtle differences between H1−Ow and H3−Ow H-bonds. Closer inspection of Figure 3 reveals that while the amplitude of the first maximum (g^{max}, Table 1) is identical for both RDFs, the amplitude associated with the first minimum (g^{min}, Table 1) for H3−Ow is significantly lower than for H1−Ow. The ratio g^{max}/g^{min} for H3−Ow is twice the ratio of H1−Ow. We interpret this feature as evidence of a more structured H-bond network around H3, indicating that the H3 atom is more tightly hydrogen bonded to water than H1. Both H1−Ow and H3−Ow hydrogen bonds are of weaker strength than the bonds in the bulk liquid (Ow−Hw), as evidenced by the corresponding g^{max}/g^{min} ratios in Table 1. Consistent with the weaker strength of the H1−Ow hydrogen bond, water molecules belonging to the second hydration shell of the solute can approach H1 at closer distances than H3 (peaks situated at ∼3.60 and ∼4.00 Å, respectively). Note also the shoulder at 3.20−3.30 Å preceding the second neighbor peak, which is more pronounced in the H3−Ow RDF.

The H5−Ow and H6−Ow RDFs (Figure 4), in contrast, do not display any first peak at short intermolecular distances. Instead, they gradually rise to a first maximum further away at 3.60 Å. Nonetheless, a broad shoulder of very low amplitude extending between ∼2.00 and ∼3.00 Å can be observed in the RDF for H6−Ow. No such structure appears in the H5−Ow RDF. This suggests that the H6 atom can form weak transient hydrogen bonds to the solvent, whereas H5 has no affinity for hydrogen bonding whatsoever. The weak H6−Ow hydrogen bonds are much longer (∼2.00−3.00 Å) compared to the bonds to the more polar amide groups (1.80−2.50 Å). Determination of a coordination number, taking, in default of a clear minimum, 2.00−3.00 Å as the coordination radius, yields $n_{H6} = 0.3$, which is much lower than n_{H1} and n_{H3}. Apart from this shoulder, the main first peak of H5−Ow and H6−Ow RDF is spread out over intervals between ∼3.00−4.00 Å and ∼3.30−4.60 Å, respectively. On the basis of the similarity of this distance to the position of the maxima of the second peaks of H1(H3)−Ow RDF (∼3.60 Å and ∼4.00 Å, respectively), the molecules in the near vicinity of H5 and H6 must be considered part of the second hydration shell of uracil.

The coordination numbers derived from the RDF for the O2−Hw and O4−Hw (Figure 5) are $n_{O2} = 1.8$ and $n_{O4} = 2.0$, i.e., the two lone pairs of the carbonyl oxygen atoms are involved in two simultaneous intermolecular H-bonds with water, on average. In addition to the marginally higher affinity to water protons ($n_{O4} > n_{O2}$), C4═O4 is also more tightly H-bonded to water compared to C2═O2, as can be inferred from the ratio g^{max}/g^{min} in O2(O4)−Hw RDF (Table 1; g^{min} is identical in both RDFs, whereas g^{max} is higher in g_{O4-Hw}). This was also observed for the N3−H3 amide group, which is adjacent to the carbonyl C4═O4 group. Again, using the g^{max}/g^{min} ratio in Table 1 as a criterion, hydrogen-bond donation by the solvent (O4−Hw, O2−Hw) leads to weaker bonding than in the bulk solvent, as was also the case when the solvent acts as acceptor (H1−Ow, H3−Ow).

Summarizing the key points of the information contained in the pair correlation functions, we find that the average total number of water molecules hydrogen bonded to the hydrophilic groups of uracil is ∼6.0. These water molecules are part of a well-defined first hydration shell coordinated with the carbonyl and amide groups. H3−Ow, O2−Hw, and O4−Hw H-bonds are of comparable strength, but always weaker than the bulk Hw−Ow hydrogen bonds. H1−Ow H-bonds are significantly weaker. Thus, the decreasing order of hydrogen bond strengths obtained here is Hw−Ow > H3−Ow > O4−Hw > O2−Hw ≫ H1−Ow.

Orientation of Hydrogen Bonds. Having investigated the statistics of hydrogen bond lengths, we continue with a characterization of angular distributions. The radial distributions correlating H atoms and an acceptor atom X = O, N are a key prerequisite for such an investigation, because the location of the minimum following the first coordination peak is generally used to specify a bonding radius r_c. The RDF analysis above shows that this gives a sharp criterion for all relevant atom pairs except for H6−Ow, where we take $r_c = 2.50$ Å (see discussion above).

Bulk solvation, however, is intrinsically three-dimensional in nature, which, for ring-shaped molecules such as uracil, can

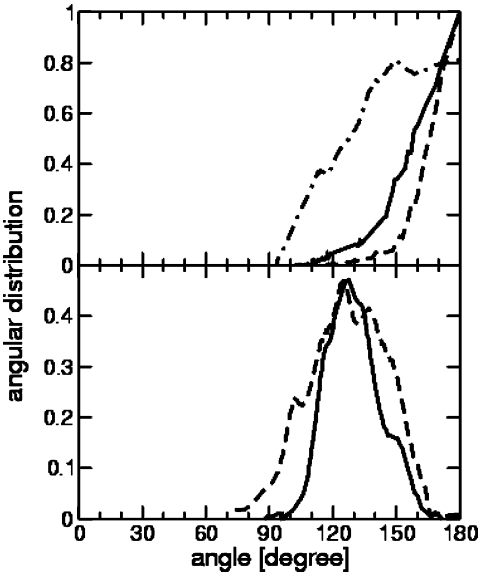

Figure 6. Distribution of angles of hydrogen bonds formed between uracil and water (linearity of H-bonds). (Top) H-atom provided by solute: N1−H1···Ow (solid), N3−H3···Ow (dashed), and C6−H6···Ow (dot−dashed). (Bottom) H atom provided by solvent: C2═O2···Hw (solid) and C4═O4···Hw (dashed). Distributions have been normalized for the sake of comparison.

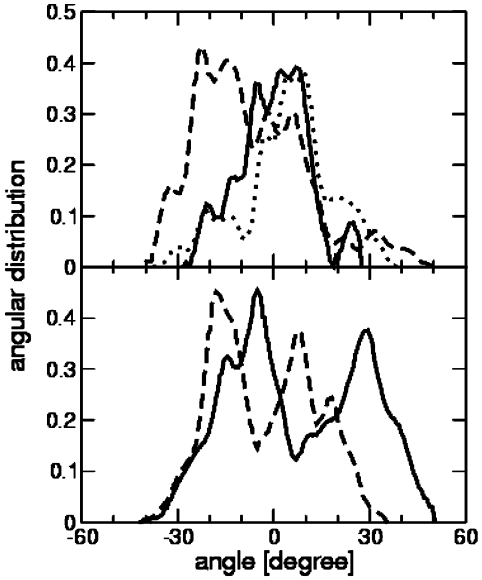

Figure 7. Angular distribution characterizing *in*-plane or *out*-of-plane orientation of uracil−water hydrogen bonds. (Top) N1−H1···Ow (solid), N3−H3···Ow (dotted), and C6−H6···Ow (dashed) H-bonds. (Bottom) C2−O2···Hw (solid) and C4−O4···Hw (dashed) H-bonds. See section 3 for the definition of the φ angle.

lead to qualitatively different types of bonding depending on the position of the solvent molecule relative to the molecular plane. We therefore have attempted to quantify the in- or out-of-plane character of H-bonds by their orientation with respect to the vector normal to the molecular plane. In particular, we will focus on the angle between the normal and the vectors H1-(H3)−Ow, O2(O4)−Hw, and H6−Ow, when the length of vectors satisfies the hydrogen-bond criterion. The complement of this angle will be denoted by φ. A zero φ value will therefore correspond to an in-plane orientation. The normal vector is generated as the cross product of two vectors specifying the plane of the ring. We estimate that fluctuations of the ring away from a perfect plane give rise to a maximum error of 5° in the values of the calculated angles.

Starting the analysis with the bond angle distributions shown in Figure 6 we first discuss the results for the amide−Ow hydrogen bonds. Hydrogen bonds to NH groups are predominantly linear with ∠N−H−Ow H-bond distributions steeply falling from a maximum at 180° and vanishing at values beyond 120°−110°. In particular, the ∠N3−H3−Ow angle shows a sharply defined linear geometry. This can be explained by (i) the stronger H3−Ow hydrogen bonds, as previously emphasized, preventing fluctuations of too big amplitude away from linearity or by (ii) geometrical hindering in the solvation shell depending on the inequivalence in position in the uracil ring: N3−H3 is flanked by two carbonyl groups both forming strong hydrogen bonds with water molecules, whereas N1−H1 is adjacent to C6−H6 with less prominent involvement in hydrogen bonding to the solvent. This suggests that water molecules H-bonded to N1−H1 have more freedom in occupying the space around N1−H1 and C6−H6 sites, allowing for larger angular deviations from linearity of H1−Ow hydrogen bonds. In contrast, water molecules hydrogen bonded to N3−H3 are more "constrained" by the immediate solvent surrounding this site having to accommodate water molecules coordinated to the adjacent C2═O2 and C4═O4 groups as well.

The narrow centering around 180° (linearity) exhibited by amide hydrogen bonding is lost for the ∠C6−H6−Ow H-bond angle (Figure 6). All angles in the range of 180°−130° occur effectively with equal probability. The very broad distribution is a reflection of the weakness of H6−Ow hydrogen bonds. We also note that, while the minimum values of ∠N−H−Ow angles are between ∼110° and 120°, which is consistent with the common definition of hydrogen bonds, a considerable fraction of ∠C6−H6−Ow angles falls outside this 120° margin and therefore should not be considered as proper hydrogen bonds.

Amide−Ow φ angle distributions are presented in Figure 7. They cover an interval between ∼−30° and ∼+30°, with narrow peaks clustering between ∼−10° and ∼+10° and ∼−5° and ∼+12° for H1−Ow and H3−Ow H-bonds, respectively. Water molecules H-bonded to amide sites are thus mostly localized in the plane of uracil, or at least not very far from it. Hydrogen bonding to C6−H6, on the other hand, tolerates a much greater diversity in position, from (approximately) *in*-plane to *out*-of-plane (with a 25°−30° uncertainty).

Carbonyl groups accept in general multiple hydrogen bonds, and as we saw from the coordination number analysis, uracil is no exception to this rule. The orientation of hydrogen bonds must adapt to this geometry and, indeed, the ∠C−O−Hw hydrogen bond angle distribution (Figure 6) displays a broad peak located in the range 120°−140°, which are values typical of a tetrahedral coordination. We note the slightly broader ∠C4−O4−Hw distribution in comparison to ∠C2−O2−Hw. This can be due to the lack of H5−Ow hydrogen bonds leaving water molecules hydrogen bonded to C4═O4 more freedom to span the space in this area. These H-bonds are mostly formed *out*-of-plane, as revealed by the φ angle distributions reported in Figure 7. A further conspicuous feature of the carbonyl φ angle distributions is that they are bimodal. The two peaks correspond to negative and positive values of the angles, signifying that the two water molecules hydrogen bonded to each carbonyl group are located on either side of the uracil plane. Moreover, the pair of water molecules is not symmetrically placed: one carbonyl−water hydrogen bond is formed not too far from the uracil plane (ϕ angles are 2°−18° for C2═O2···Hw and 0°∠11° for C4═O4···Hw H-bonds), whereas the other carbonyl−water H-bond is strictly formed *out*-of-plane (φ angles

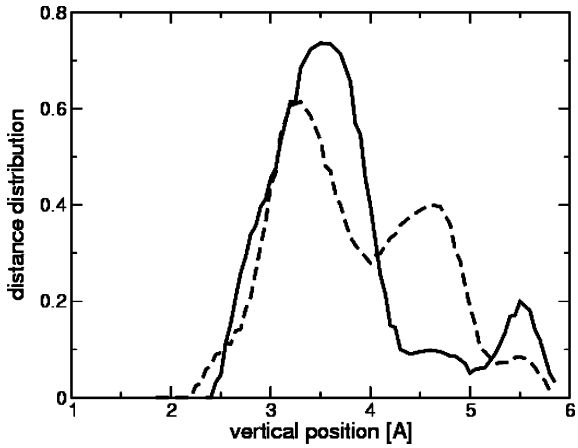

Figure 8. Distributions of water Ow (solid) and Hw (dotted) vertical positions above the uracil ring. See text section 4 for definitions. Distances span the interval 0 and 5.75 Å (corresponding to half-box size).

are 11°−21° and 23°−30°, respectively for C2═O2···Hw and C4═O4···Hw H-bonds). The small differences between the carbonyl groups again must be related to the proximity to the defect in the hydrogen-bonded network created by the C5−H5 site.

Out-of-Plane van der Waals Contacts. We complete the description of the first hydration shell of uracil by examining the solvent molecules that belong to the first hydration shell of the solute, but do not form hydrogen bonds with the donor or acceptor sites of uracil. These molecules are situated above and below the molecular plane. To identify these out-of-plane molecules, we define a circular region with the center of uracil ring as the origin. The radius of the circle is 1.50 Å, which corresponds to the average separation of ring atoms (N1, C2, N3, C4, C5, and C6 in Figure 2; see also Figure 1 of paper I) from the center. Projecting the atomic positions of water molecules on the molecular plane, we record the height of Ow and Hw atoms if their projected coordinates fall inside the circle. While the choice of the radius of 1.5 Å is somewhat arbitrary, an upper bound is set if double counting of molecules in the hydration shell is to be avoided. For example, with a radius 2.00 Å we would already include solvent molecules H-bonded to the carbonyl groups. These molecules were considered above as part of the in-plane section of the first hydration shell.

The height distribution generated by this procedure is given in Figure 8. Out-of-plane molecules appear to be organized in layers with the Ow atoms of the first layer coming in at distances between 2.40 and ∼4.00 Å. Considering the van der Waals radii of the atoms, we conclude that there is no room for an exclusion volume around the uracil ring. We find that this first layer is constituted of a maximum of three water molecules, with an average between one and two water molecules. These weakly bonded out-of-plane water molecules complete the first hydration shell of uracil, which, together with the six solvent molecules hydrogen bonded to the donor and acceptor sites, is thus composed of at most nine water molecules. Typical configurations are displayed in Figure 9.

Two more out-of-plane hydration layers can be distinguished in Figure 8: Solvent molecules separated from the molecular ring by Ow height values ranging from ∼4.00 to ∼5.00 Å are part of the second hydration shell. Vertical projections from ∼5.00 to ∼5.75 Å (half-box width) correspond to water molecules of the third hydration shell. Moreover, differentiating between Ow and Hw sites, we see the same general pattern, with the distribution for Hw being shifted toward smaller distances. The minimum distance of Hw to the molecular plane is 2.20 Å, while the minimum for Ow is 2.40 Å. Thus, water molecules above and below the uracil ring have a slight tendency to approach the ring with the hydrogen atoms down. This would suggest some kind of hydrogen bonding to uracil through its π-cloud. In particular, the first peak in Ow height distribution obtained here is centered around the value of 3.40 Å, which is comparable to the distance separating the center of mass of benzene and the oxygen atom of the water molecule in the prototypical benzene−water complex.[48−51]

Intramolecular Structure. The response of the uracil geometry to solvation has been discussed in paper I (the numbers are listed in Table 1 of that publication[15]). Summarizing these results, we observed that amide bonds are stretched by +0.022 Å for N1−H1 and +0.018 Å for N3−H3. The C4═O4 bond with a increase of +0.025 Å was found to be slightly longer compared to C2═O2, which increased by +0.018 Å. The slightly higher number of water molecules coordinated to C4═O4, as well as more tight H-bonds to this site, are a likely explanation for this differentiation between carbonyl bonds. The C5−H5 and C6−H6 distances showed no response to solvation. These structural changes seem consistent with the observed hydrogen-bond patterns. A further effect of solvation worth mentioning is the substantial overall contraction of the uracil ring amounting to reductions up to 0.020 Å of N−C and (single) C−C bond lengths.

We have also analyzed the intramolecular geometry of the water molecules, i.e., Ow−Hw bond lengths and ∠Hw−Ow−Hw bond angles. The purpose here was to examine whether the water molecules of the first hydration shell, and in particular the subset directly H-bonded to the solute, have internal geometries that differ from the water molecules of the outer hydration shells and also from bulk liquid. To this end, we have given in Table 2 the average (av), the most probable (max corresponding to the maximum of the distributions), the minimum (bmin), and maximum (bmax) values of Ow−Hw and ∠Hw−Ow−Hw as measured over the aqueous trajectory. A comparison is also made to the values of an isolated water molecule (optimized in this work). The data in Table 2 immediately verify that there are no significant distinctions between water molecules hydrogen bonded to the hydrophilic sites of uracil and water molecules of the other solvation shells. The average value of the Ow−Hw bond length is identical in both cases, and the only subtle variation comes from the most probable Ow−Hw bond length, which is increased by 0.003 Å when the water molecules are hydrogen bonded to uracil. Similarly, we observe a slight increase of 1° of the most probable ∠Hw−Ow−Hw bond angle when the water molecules are H-bonded to uracil. This is in contrast to simulations of the solvation of small or multiply charged ions. However, in our case, we are dealing with a neutral solute immersed in water: the strength of uracil−water H-bonds is always less than the hydrogen bonding in the solvent itself and, hence, not large enough to perturb the internal water geometry.

5. Relaxation Dynamics

Rearrangement and Relaxation Dynamics. A time window of ≈8 ps is (just) sufficient to observe dynamical reorganizations of water molecules in the first hydration shell of uracil. Water molecules could be seen to move from the first to the second solvation layer and vice versa. They also exchanged between hydrophilic sites while essentially remaining hydrogen bonded to uracil. The duration of the simulation is too short to determine the residence time of water molecules in the first hydration shell.

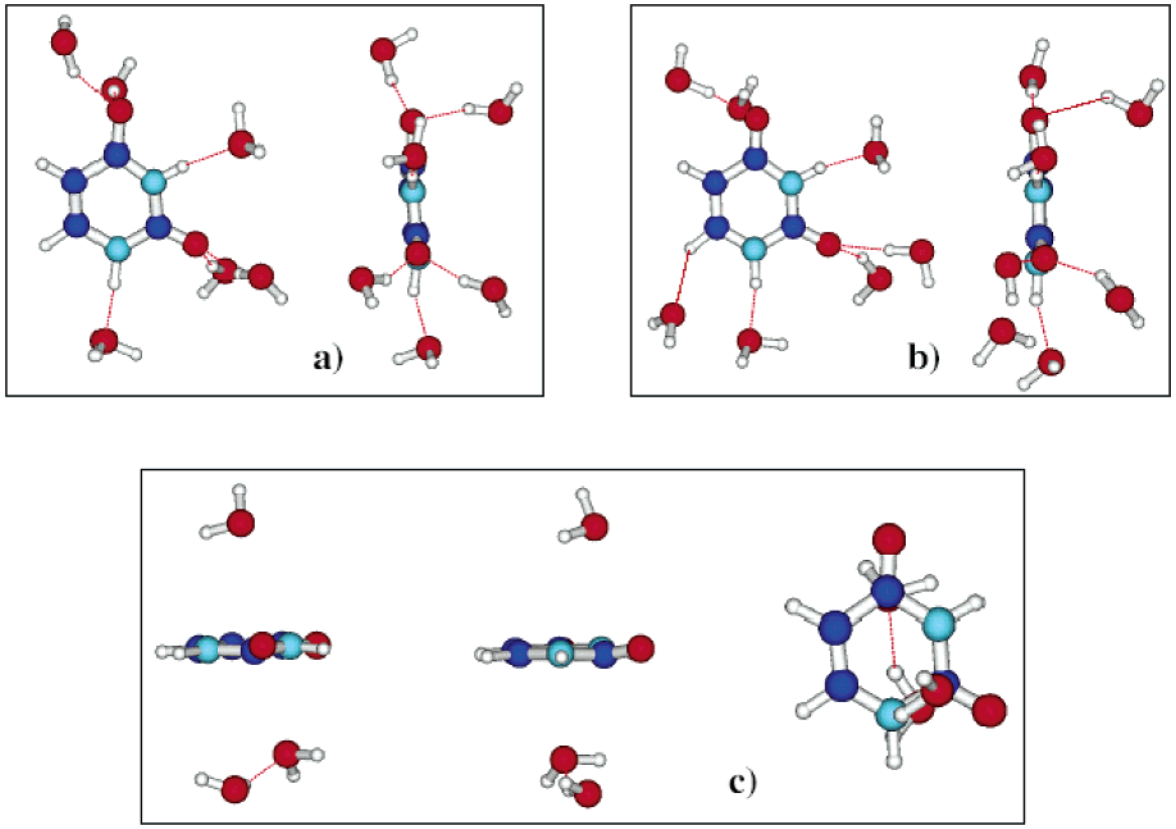

Figure 9. Typical configurations of the first hydration shell of uracil, sampled from the dynamics in solution. The figure highlights hydrogen-bonding patterns of selected molecules (for clarity the other molecules have been suppressed). Two typical configurations illustrating H-bonding to the hydrophilic sites composed of six (a) and seven (b) solvent molecules (views from above the uracil ring and from the side). (c) Configuration showing three water molecules in out-of-plane coordination (three different views of the same configuration).

TABLE 2: Structural Parameters of Water Solvent Molecules

	H-bonded[a]	other[b]	all[c]	H_2O (vac)[d]
r_{OwHw}^{av}	1.002	1.002	1.002	0.982
r_{OwHw}^{max}	1.001	0.998	0.998	0.982
$R_{OwHw}^{bmin}/R_{OwHw}^{bmax}$	0.903/1.158	0.903/1.164	0.903/1.164	
$\angle$Hw−Ow−Hw^{av}	105.4	105.0	105.0	103.8
$\angle$Hw−Ow−Hw^{max}	105.0	104.0	104.0	103.8
$\angle$Hw−Ow−Hw$^{bmin}/\angle$Hw−Ow−Hw^{bmax}	84.0/125.0	80.0/133.2	80.0/133.2	

[a] Hydrogen bonded to N−H, C═O, and C6−H6 sites. [b] Not hydrogen bonded to uracil. [c] Average over all 49 water molecules of the sample. [d] Equilibrium water monomer at 0 K. Listed are the average (r_{OwHw}^{av}) and the most probable (r_{OwHw}^{max}) OwHw intramolecular bond length (in Å) and the average ($\angle$Hw−Ow−Hw^{av}) and the most probable ($\angle$Hw−Ow−Hw^{max}) Hw−Ow−Hw internal bond angle. Also reported: minimum and maximum values over the full length of the MD trajectory (r_{OwHw}^{bmin} and r_{OwHw}^{bmax} for bond lengths, $\angle$Hw−Ow−Hw^{bmin} and $\angle$Hw−Ow−Hw^{bmax} for angles).

It is also too short for a proper determination of lifetimes of solute−solvent hydrogen bonds. Such a quantitative analysis comparing the relaxation dynamics of the different hydrophilic groups (N−H, C═O, and C6−H6) would have been very instructive but is unfortunately not feasible on our time scale. We can only state that hydrogen bonds between water molecules and uracil (whatever the site) can last from a few hundreds of femtoseconds (200−500 fs) to a few picoseconds (2.0−5.0 ps).

With regard to the relaxation in the bulk solvent, we are in a better position. Previous work[46,47] has shown that comparable ab initio MD system sizes and time scales (≈10 ps) allow for a rough estimate of the self-diffusion constant and reorientation times, although the uncertainties are high (20−30%). Accordingly, the self-diffusion coefficient of the water molecules was computed from the mean square displacement of the water oxygen atoms. The data are plotted in Figure 10. We obtain a value of $D = 0.10$ Å^2 ps^{-1}. The diffusion is therefore slower than the $D = 0.28$ Å^2 ps^{-1} estimate of Silvestrelli and Parinello[46] for their 10 ps 64-molecule trajectory of pure liquid water using the same BLYP density functional as applied here (the experimental value for liquid water[52] is $D = 0.24$ Å^2 ps^{-1}). We have also calculated the time autocorrelation of the orientation of the water molecular symmetry axis, and the correlation of the vector connecting the Hw atoms. Results are also displayed in Figure 10: Shown are the logarithm of the decay of the $l = 1$ spherical harmonic of the symmetry vector and the logarithm of the $l = 2$ function of the vector linking the Hw atoms averaged over all water molecules. We obtain characteristic times of $\tau_d = 7$ ps and $\tau_{HH} = 5$ ps, respectively for the molecular symmetry axis and the Hw−Hw vector orientational correlations. These values are approximately a factor of 2 slower than the times previously obtained in the simulation of deuterated D_2O liquid.[53] The experimental estimate for pure liquid water is $\tau_{HH} = 2$ ps (NMR measurements[54]), hence also faster than the value calculated here for the water solvent.

The main point of this exercise is that in default of a reliable estimate of pressure (for technical reasons determination of the pressure is too demanding in terms of computational costs), the

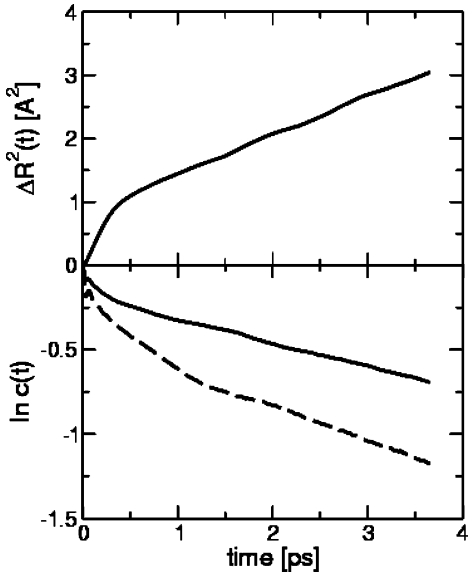

Figure 10. (Top) mean square displacement of oxygen atoms of solvent water molecules as a function of time. Result is averaged over all water molecules. Fitting of the time dependency in the 1−3.5 ps interval to a straight line gives an estimated self-diffusion coefficient of $D = 0.10$ Å^2 ps^{-1}. (Bottom) logarithm of the orientational time correlation function of a vector fixed in a molecule of water. Relaxation of the $l = 1$ correlation of the molecular symmetry axis (solid line), and relaxation of the $l = 2$ correlation of the vector connecting the Hw atoms (dashed line). Results are averaged over all water molecules. Characteristic times τ_d (with $l = 1$) and τ_{HwHw} (with $l = 2$) are obtained by fitting the time dependency to straight lines omitting the first picosecond yielding the values $\tau_d = 7$ ps respectively $\tau_{HH} = 5$ ps (statistical uncertainties are in the order of 30%).

self-diffusion and orientational relaxation can be used as a probe of the effective thermodynamic state. Coupling to the solute can be expected to have some effect. Indeed, an estimate of τ_{HH} for the water molecules hydrogen bonded to uracil gave Hw−Hw relaxation times slightly faster than the rest of the solvent (3−4 ps), consistent with the weaker hydrogen bonding in the first solvation shell. However, measured over all solvent the influence of the solute is small. Any major deviation from the relaxation dynamics of the bulk liquid is therefore more likely due to the model system containing the wrong number of solvent molecules. One water molecule more or less in a fixed volume of the size used in ab initio MD can cause significant changes in the pressure (on the order of hundreds of bar). The 50% reduction of diffusion and reorientation rates can therefore be interpreted as a confirmation that the thermodynamic state is not too far from ambient conditions.

6. Comparison to Gas-Phase Hydration

Structures found by geometry optimization of hydrated uracil in the gas-phase are often preconditioned by the starting configurations. For example, the calculations of refs 23, 30, 35, 37, and 38 have been mainly directed at structures in which the water molecules form hydrogen bonds located in the average plane defined by the uracil ring. Within this "restriction" the configurations of lowest energy turned out to systematically involve water dimers hydrogen bonded to two adjacent donor and acceptor sites.[23,35,38] In particular, the configurations of water dimers bridging adjacent groups (N1−H1, C2═O2) or (N3−H3, C4═O4) observed in the U·7H_2O study of refs 37 and 38 proved to be energetically more favorable than binding of water monomers to the same adjacent sites.

In view of the finite temperature (310 K in our simulation) and the natural three-dimensional H-bonding network of the water solvent, the question arises whether these states will be stable in aqueous uracil, where they have to compete with new types of hydrogen bonding. Now water molecules in the first solvation shell have the option to form the maximum number of hydrogen bonds to the bulk liquid or be associated among themselves and participate in the bulk network as dimeric entities attached to the solute. To answer this question, we have investigated the possible occurrence of dimers H-bonded to two consecutive sites of uracil during the dynamics. Again, water−water hydrogen bonds are defined on the basis of a maximum Hw−Ow intermolecular distance, 2.50 Å, and ∠Hw−Ow−Hw or ∠Ow−Hw−Ow H-bond angles in the range 120°−180°. We found that binding of water dimers to uracil is relatively rare: an average fraction of only 0.2 water dimers measured over the 7.3 ps trajectory falls in this category. When this happens, very distorted water dimer geometries were obtained: H-bond angles were in the range 120°−130°, and intermolecular distances were close to 2.30−2.50 Å. Very surprisingly, the only exception concerns water dimers that were found hydrogen bonded to the adjacent C6−H6 and N1−H1 sites. In that case, the resulting geometry was very similar to that of the isolated dimer.

Analysis of lifetimes of transient water dimers in the first hydration shell further supported this picture. From a record of the cumulative time spent by water dimers H-bonded to two adjacent donor and acceptor sites, we found, in increasing order, 102 fs time length for dimer bridges between the N1−H1 and C2═O2 groups, 218 fs between N1−H1 and C6−H6, 240 fs between N3−H3 and C4═O4, and 893 fs between N3−H3 and C2═O2. Considering the strength of uracil−water H-bonds previously discussed, it is perhaps not surprising that the longer durations found here involved N3−H3 and the carbonyl groups.

In conclusion, in solution water molecules appear to prefer binding to the hydrophilic sites of uracil as monomers. The explanation must be that this leaves more freedom to form H-bonds with the bulk water molecules, resulting in a better stabilization of the collective water−water H-bond network. With only one hydrogen bond to a solute site, the water molecules in the first solvation shell seem to be able to be accommodated in the surrounding solvent with a minimum of perturbation of the regular tetrahedral hydrogen bonding pattern in the liquid. This is why the average length of hydrogen bonds between solvent molecules (≈1.70−1.75 Å; see Figure 1 and Table 1) is practically identical to the value in the pure solvent (which is, incidently, also very close to the hydrogen bonding in the coordinated dimers found in the clusters calculations[38]). Similarly, monomers are not shared between two adjacent sites of uracil, i.e., do not form two simultaneous hydrogen bonds with a pair of consecutive donor and acceptor sites of uracil. This excludes the appearance of the water monomer bridge suggested in some geometry optimizations of U·$n_w H_2O$ complexes.[23,28,37,38]

The cooperative nature of hydrogen bonding in water is probably also the explanation of the apparent conflict between the relative strength of the hydrogen bonds to the H1 and H3 site and the gas-phase acidity of these two groups. Computations have shown that the deprotonation energy of the N1−H1 bond (in the gas phase) is about 45 kJ mol^{-1} less compared to the N3−H3 bond, suggesting that the affinity for hydrogen bonding of H1 should be higher (see, for example, ref 28). However, as discussed in section 4, our simulations indicate that the coordination to H3 is more structured compared to H1, which

we interpreted as the result of formation of stronger bonds with the solvent. This contrast between H1 and H3 was rationalized in terms of the geometry of uracil. We argued that N3−H3 may be able to benefit from its position between C4═O4 and C2═O2, both of which are good hydrogen-bond acceptors. N1−H1, on the other hand, is flanked by a hydrophilic group (C2═O2) and an essentially hydrophobic group (C6−H6), which may lead to a local solvent structure less conducive to hydrogen bonding. One may speculate, therefore, that these collective structural effects give N3−H3 an advantage that is able to overcome the difference in the polarity with respect to the N1−H1 bond.

7. Summary and Conclusions

Summary of Results. The objective we have set for the present paper was to give a detailed account of the performance of DFT-based ab initio MD in describing the hydration of a small but realistic model system, representative of the aqueous organic molecule of biochemical importance. The model we chose, mainly for its compactness, is the simplest nucleic acid base, uracil. One aim was to extract from the molecular dynamics trajectory a precise description of the structural and dynamical properties of the solvent surrounding the uracil molecule. The same microscopic data were used in a previous publication[15] (paper I) to calculate the infrared spectrum of aqueous uracil, which then could be correlated to the results of the structural and vibrational analysis, arriving at an interpretation of the spectrum.

The broad picture of the hydration of uracil emerging from the ab initio MD simulation conforms to what is known or can be anticipated for this class of aqueous molecules. Amide and carbonyl groups participate fully in solute−water intermolecular hydrogen bonding. Bond lengths show the regular variation from 1.70 Å, 1.80 Å to 2.30, 2.50 Å, measured from the first peak in the radial distribution to the next minimum, leading to one bond per amide H and two bonds per carbonyl O atom. The C5−H5 group is not involved in hydrogen bonding, and the closest water molecules to this site belong to the second hydration shell of the solute. The other CH group, C6−H6, however, showed a hint of hydrogen bonding with very long (2.40−2.50 Å), distorted (110°−120°), and short-lived bonds. The average number of solvent molecules hydrogen bonded to the main hydrophilic sites of uracil is six. In addition, the full first hydration shell contains a maximum of three water molecules positioned in van der Waals contact above and below the uracil ring. Also this predominantly hydrophobic coordination shows some directional preference, suggesting a weak attraction of the water H atoms to the electronic π cloud. In view of the biological function of nucleic bases, we have also searched for differences in hydrogen bonding to the two NH and C═O groups, depending on their position in the ring, in particular the proximity to the C═C bond. On the basis of the features of the radial distribution functions, we found that the N3−H3 and C4═O4 groups, which are next to each other, form the strongest bonds. Bonding to C2═O2 is only marginally weaker, while the N1−H1 has a significantly lower hydrogen bond affinity.

In contrast to quantum chemistry calculations based on optimization of specific preselected geometries of vacuum clusters, the open three-dimensional structure of the first hydration shell in the MD simulation is stabilized by interactions with the bulk solvent. To illustrate this important distinction, we showed that a frequently observed structural motive of vacuum coordination shells, water dimers bridging adjacent donor and acceptor sites,[23,35,38] plays no role in solution, where hydrogen bonding to the solute essentially only involves water monomers. Similarly, the weak H-bonds to CH groups found in clusters are eliminated by the finite temperature and competition with the bulk solvent. In this context, we further note that our results also contradict previous claims[31,55] that only three water molecules can be accommodated in the first hydration shell of uracil.

Evaluation of Ab Initio MD Methods. Modeling of a finite-temperature extended-solvent environment in full electronic detail comes, of course, at a computational price, and one could argue that this price includes compromising on accuracy. The good agreement we obtained in paper I for IR intensities and band shapes can be taken as (indirect) experimental support for the validity of results for structure and dynamics. However, as pointed out in the Introduction, ab initio MD simulation is, in practice, a compromise between system size and run length, which, contingent on the computational resources available, also evolves in the course of time. Thus, the first studies of (pure) liquid water[53,56,] used small system sizes (32 H_2O molecules in a periodic simple cubic cell) with a typical run length (2−5 ps), which was just the very minimum required to observe important dynamical processes characteristic for liquid water, such as hydrogen-bond breaking and rearrangement (≈2−3 ps) and hopping of excess protons in acids (≈1−2 ps).[57,58] Within these constraints, the BLYP[42,43] functional (as also applied here) was found to give good agreement with experimental data for structure and dynamics. Subsequent work[46,47] extended the duration of the simulation to 10 ps and system dimensions to 64 molecules and consolidated the early results. These calculations also gave an indication of size effects, in particular on the self-diffusion, which was found to become faster in the larger system. Also, the effect of zero-point motion has been investigated in an ab initio path integral MD study of the 64-molecule model system.[59] Staying within the same regime of length and time scales, it was shown in ref 60 that also PBE[61] (a GGA similar to BLYP, but based on a first principle parametrization) is suitable for the modeling of liquid water.

Studies of the solvation of molecules and ions have followed the same progression in length and time scales, initially using model systems consisting of a single solute immersed in a cell containing a quantity of solvent similar to the early pure liquid tests (only about 30 H_2O molecules). Because of the relevance for the hydration of uracil, we mention here calculations for aqueous methanol,[62] ammonium,[63] and DMSO[64] (for further references and examples of inorganic aqueous species, see ref 15 and a recent review paper by Tuckerman[65]). One of the first detailed investigations of an aqueous solute of direct biological interest was the study of the hydration of a sugar molecule (glucose) by Molteni and Parrinello.[66] This more bulky species requires a larger number of solvent molecules (58) to build a complete first and second solvation shell in a cubic period cell. Uracil is (roughly) of the same size, and we have used also a MD cell with similar dimensions (11.5 Å), which is therefore comparable to the system parameters of the pure water studies of refs 46 and 47. Also, the duration of the runs (≈10 ps) is in the range of the time scale of these more recent extended bench mark studies of liquid water.

These and other studies have helped establish the Car−Parrinello method, in the implementation used here, as a new tool in computational chemistry opening up the possibility of examining reactive events in aqueous solution in all atomic detail and even, in some case, a computation of thermochemical constants could be carried out.[67] However, this picture has recently been questioned by new investigations pushing the

frontiers of system size, run length, and other convergence parameters (such as the number of plane waves and fictitious mass) further back[68] or using alternative more expensive schemes for maintaining adiabaticity (Born−Oppenheimer dynamics).[69,70] These results seem to indicate that the minimum 32 H_2O molecule BLYP model system is a metastable liquid. This could mean that given enough time to equilibrate the system will settle in a more structured state with a slower relaxation dynamics. The final verdict is still uncertain, as is the effect on the larger 64 molecule system, which is similar in size to the model used in this study. However, even if it turns out that the Car−Parrinello studies of aqueous systems to date have benefited from a cancellation of errors (not uncommon in computational chemistry), the results of the present and numerous other simulations are evidence that this scheme, in a more empirical sense, represents a sufficiently accurate and computationally efficient model of aqueous solutions that can be used to study the hydration of complex organic molecules.

Acknowledgment. The authors would like to thank CINES (Montpellier, France) and CCR (Jussieu, Paris) for generous access to their computational facilities. Part of the calculations were performed on the beowulf cluster of the CSE group at Daresbury Laboratories (UK) as part of a CCP1 flagship project. M.P.G acknowledges the ESF Scientific Program on "Challenges in molecular simulations: bridging the length and time scale gap (SIMU)" for a fellowship. We are also thankful to I. Tavernelli for his help in setting up the model system.

References and Notes

(1) Foloppe, N.; MacKerell, A. D. *J. Comput. Chem.* **2000**, *21*, 86.
(2) MacKerell, A. D.; Banavali, N. K. *J. Comput. Chem.* **2000**, *21*, 105.
(3) Cheatham, T. E.; Cieplak, P.; Kollman, P. A. *J. Biomol. Struct. Dyn.* **1999**, *16*, 845.
(4) Auffinger, P.; Westhof, E. *J. Mol. Biol.* **1997**, *269*, 326.
(5) Auffinger, P.; Westhof, E. *J. Mol. Biol.* **2001**, *305*, 1057.
(6) Karplus, P. A.; Faerman, C. H. *Curr. Opin. Struct. Biol.* **1994**, *4*, 770.
(7) Rudnicki, W. R.; Pettitt, B. M. *Biopolymers* **1997**, *41*, 107.
(8) Makarov, V.; Pettitt, B. M.; Feig, M. *Acc. Chem. Res.* **2002**, *35*, 376.
(9) Iuchi, S.; Morita, A.; Kato, S. *J. Phys. Chem. B* **2002**, *106*, 3466.
(10) Car, R.; Parrinello, M. *Phys. Rev. Lett.* **1985**, *55*, 2471.
(11) King-Smith, R. D.; Vanderbilt, D. *Phys. Rev. B* **1993**, *47*, 1651.
(12) Vanderbilt, D.; King-Smith, R. D. *Phys. Rev. B* **1993**, *48*, 4442.
(13) Silvestrelli, P. L.; Bernasconi, M.; Parrinello, M. *Chem. Phys. Lett.* **1997**, *277*, 478.
(14) Zhu, Z.; Tuckerman, M. E. *J. Phys. Chem. B* **2002**, *106*, 8009.
(15) Gaigeot, M.-P.; Sprik, M. *J. Phys. Chem. B* **2003**, *107*, 10344.
(16) Port, G. N. J.; Pullman, A. *FEBS. Lett.* **1973**, *31*, 70.
(17) Pullman, B.; Miertus, S.; Perahia, D. *Theor. Chim. Acta (Berlin)* **1979**, *50*, 317.
(18) Del Bene, J. E. *J. Comput. Chem.* **1981**, *2*, 188.
(19) Aamouche, A.; Berthier, G.; Cadioli, B.; Gallinella, E.; Ghomi, M. *J. Mol. Struct. (THEOCHEM)* **1998**, *426*, 307.
(20) Ghomi, M.; Aamouche, A.; Cadioli, B.; Berthier, G.; Grajcar, L.; Baron, M. H. *J. Mol. Struct.* **1997**, *411*, 323.
(21) vanMourik, T.; Price, S. L.; Clary, D. C. *J. Phys. Chem. A.* **1999**, *103*, 1611.
(22) vanMourik, T.; Benoit, D. M.; Price, S. L.; Clary, D. C. *Phys. Chem. Chem. Phys.* **2000**, *2*, 1281.
(23) vanMourik, T. *Phys. Chem. Chem. Phys.* **2001**, *3*, 2886.
(24) Chandra, A. K.; Nguyen, Zeegers-Huyskens, T. *J. Phys. Chem.* **1998**, *102*, 6010.
(25) Chandra, A. K.; Nguyen, M. T.; Uchimaru, T.; Zeegers-Huyskens, T. *J. Phys. Chem.* **1999**, *103*, 8853.
(26) Chandra, A. K.; Nguyen, M. T.; Zeegers-Huyskens, T. *J. Mol. Struct.* **2000**, *519*, 1.
(27) Chandra, A. K.; Nguyen, M. T.; Uchimaru, T.; Zeegers-Huyskens, T. *J. Mol. Struct.* **2000**, *555*, 61.
(28) Nguyen, M. T.; Chandra, A. K.; Zeegers-Huyskens, T. *J. Chem. Soc., Faraday Trans.* **1998**, *94*, 1277.
(29) Dolgounitcheva, O.; Zakrzewski, V. G.; Ortiz, J. V. *J. Phys. Chem.* **1999**, *103*, 7912.
(30) Smets, J.; McCarthy, W. J.; Adamowicz, L. *J. Phys. Chem.* **1996**, *100*, 14655.
(31) Smets, J.; Smith, D. M. A.; Elkadi, Y.; Adamowicz, L. J. *Phys. Chem. A.* **1997**, *101*, 9152.
(32) Gorb, L.; Leszczynski, J. *Int. J. Quantum Chem.* **1997**, *65*, 759.
(33) Aleman, C. *Chem. Phys.* **1999**, *244*, 151.
(34) Aleman, C. *Chem. Phys.* **1999**, *302*, 461.
(35) Gadre, S. R.; Babu, K.; Rendell, A. P. *J. Phys. Chem. A.* **2000**, *104*, 8976.
(36) Shiskin, O. V.; Gorb, L.; Leszczynski, J. *J. Phys. Chem. B.* **2000**, *104*, 5357.
(37) Gaigeot, M. P.; Ghomi, M. *J. Phys. Chem. B.* **2001**, *105*, 5007.
(38) Gaigeot, M. P.; Kadri, C.; Ghomi, M. *J. Mol. Struct.* **2001**, *565*−*566*, 469.
(39) Marx, D.; Hutter, J. *Ab initio molecular dynamics: theory and implementation, in Modern methods and algorithms of quantum chemistry*; Grotendorst, J., Ed.; John von Meumann Institute for Computing: Julich, NIC Series, 2000; Vol 1, pp 301−449.
(40) Trouillier, N.; Martins, J. L. *Phys. Rev. B* **1991**, *43*, 1993.
(41) Kleinman, L.; Bylander, D. M. *Phys. Rev. Lett.* **1982**, *48*, 1425.
(42) Becke, A. *Phys. Rev. A* **1988**, *38*, 3098.
(43) Lee, C.; Yang, W.; Parr, R. G. *Phys. Rev. B* **1988**, *37*, 785.
(44) Vuilleumier, R.; Sprik, M. *J. Chem. Phys.* **2001**, *115*, 3454.
(45) Hutter, J.; Parrinello, M.; et al. *CPMD*, version 3.4.1; IBM Research Division, MPI Festkoerperforschung: Stuttgart.
(46) Silvestrelli, P. L.; Parrinello, M. *J. Chem. Phys.* **1999**, *111*, 3572.
(47) Izvekov, I.; Voth, G. A. *J. Chem. Phys.* **2002**, *116*, 10372.
(48) Karlstrom, G.; Linse, P.; Wallqvist, A.; Jonsson, B. *J. Am. Chem. Soc.* **1983**, *105*, 3777.
(49) Suzuki, S.; Green, P. G.; Bumgarner, R. E.; Dasgupta, S.; Goddard, W. A.; Blake, G. A. *Science* **1992**, *257*, 992.
(50) Gregory, J. K.; Clary, D. C. *Mol. Phys.* **1996**, *88*, 33.
(51) Courty, A.; Mons, M.; Dimicoli, I.; Piuzzi, F.; Gaigeot, M. P.; Brenner, V.; de Pujo, P.; Millie, Ph. *J. Phys. Chem.* **1998**, *102*, 6590.
(52) Krynicki, K.; Green, C. D.; Sawyer, D. W. *Faraday Discuss. Chem. Soc.* **1978**, *66*, 199.
(53) Sprik, M.; Hutter, J.; Parrinello, M. *J. Chem. Phys.* **1996**, *105*, 1142.
(54) Jonas, J.; DeFries, T.; Wilber, D. J. *J. Chem. Phys.* **1976**, *65*, 582.
(55) Chahinian, M.; Seba, H. B.; Ancian, B. *Chem. Phys. Lett.* **1998**, *285*, 337.
(56) Laasonen, K.; Sprik, M.; Parrinello, M.; Car, R. *J. Chem. Phys.* **1993**. *99*, 9080.
(57) Tuckerman, M.; Laasonen, K.; Sprik, M.; Parrinello, M. *J. Chem. Phys.* **1995**, *103*, 150.
(58) Marx, D.; Tuckerman, M.; Hutter, J.; Parrinello, M. *Nature* **1999**, *397*, 601.
(59) Chen, B.; Ivanov, I.; Klein, M. L.; Parrinello, M. *Phys. Rev. Lett.* **2003**, *91*, 215503.
(60) Schwegler, E.; Galli, G.; Gygi, F.; Hood, R. Q. *Phys. Rev. Lett.* **2002**, *87*, 265501.
(61) Perdew, J. P.; Burke, K.; Ernzerhof, *Phys. Rev. Lett* **1996**, *77*, 3865.
(62) Van Erp, T. S.; Meijer, E. J. *Chem. Phys. Lett.* **2001**, *333*, 290.
(63) Bruge, F.; Bernasconi, M.; Parrinello, M. *J. Am. Chem. Soc.* **1999**, *121*, 10833
(64) Kirchner, B.; Hutter, J. *Chem. Phys. Lett.* **2002**, *364*, 497.
(65) Tuckerman, M. *J. Phys.: Condens. Matter* **2002**, *14*, R1297.
(66) Molteni, C.; Parrinello, M. *J. Am. Chem. Soc.* **1998**, *120*, 2168.
(67) Davies, J. E.; Doltsinis, N. L.; Kirby, A. J.; Roussev, C. D.; Sprik, M. *J. Am. Soc. Chem.* **2002**, *124*, 6594.
(68) Grossman, J. C.; Schwegler, E.; Draeger, E. W.; Gygi, F.; Galli, G. *J. Chem. Phys.* **2003**, *120*, 516.
(69) Vassilev, P.; Hartnig, C.; Koper, M. T. M.; Frechard, F.; van Santen, R. *J. Chem. Phys.* **2001**, *115*, 9815.
(70) Asthagiri, D.; Pratt, L. R.; Kress, J. D. *Phys. Rev. E* **2003**, *68*, 041505.